2017

Glaciovolcanic Megapillows of Undirhliðar, Reykjanes Peninsula, Southwestern Iceland

Rachel Heineman
Oberlin College

GLACIOVOLCANIC MEGAPILLOWS OF UNDIRHLÍÐAR, REYKJANES PENINSULA, SOUTHWESTERN ICELAND

Rachel Heineman

Honors Research in Geology

Dr. F. Zeb Page, Thesis Advisor

Oberlin College

2016-2017

ABSTRACT

At Undirhlíðar tindar on the Reykjanes Peninsula, southwestern Iceland, megapillows are among the features formed during a series of ridge-building glaciovolcanic eruptions. Mapping of the northeastern 3 km of the ridge and petrographic and geochemical analysis of the megapillow outcrops occurring throughout this area demonstrate their role in the multi-stage construction of the ridge modeled by Pollock et al. (2014). The outcrops exhibit radial jointing, bands of vesicles and glassy rims; they occur in high relief surrounded by basalt breccia resembling pillow rubble, and are composed of plagioclase-phyric olivine basalt with plagioclase-rich groundmass. They occur in multiple pillow lava units formed from two distinct magma batches. Two groups of outcrops are represented that are petrographically, geochemically and geographically distinct; the first group is near to and consistent with the pillow units of Undirhlíðar quarry described by Pollock et al. (2014), and the second group, located near the tephra cone, is derived from a more evolved unit of the same magma. Megapillows show significant plagioclase accumulation with variable phenocryst zoning, indicating the movement of multiple pulses of magma through the megapillows. Megapillows at Undirhlíðar may represent a significant mechanism, demonstrated elsewhere at a marine megapillow by Goto and McPhie (2004), for magmatic distribution: feeding and then overrunning pillows which propagate and are fed from their basal margins at the eruptive front.

INTRODUCTION

Pillow lavas are among the most common lava morphologies on Earth, yet the construction of pillow-dominated volcanoes is not widely understood due to the relative inaccessibility of the submarine environments in which they form. Although the vast majority of pillow lavas erupt along mid-ocean ridges at the bottom of the sea (e.g. Batiza and White 2000, Furnes et al. 2007, Johns et al. 2006, Walker 1992) or in lakes (e.g. McClintock et al. 2008), subglacial volcanoes, which form by eruption in subglacial lakes and are exposed following glacial retreat (e.g. Edwards et al. 2009, Höskuldsson et al. 2006, Jones 1969), allow us to study pillow-dominated volcanoes at the Earth's surface and investigate the eruptive processes that control their development. In addition, the products of subglacial volcanism may be used in the study of Earth's paleoclimate to address outstanding questions regarding pre-Last Glacial Maximum (LGM) ice sheets. Subglacial volcanic edifices are generally more resistant to erosion than other glaciogenic deposits (i.e. till), the evidence of which was largely destroyed during the LGM (Fulton 1992, Jackson et al 1996, Barendegt and Irving 1998), and can provide constraints as to the extent and thicknesses of pre-LGM terrestrial glaciers (Edwards et al 2009). Efforts to better understand subglacial volcanism may therefore allow critical insight into historical patterns of glaciation as well as the development of Earth's seafloor.

General models for the formation of basaltic glaciovolcanoes show a single period of effusive pillow formation followed by a transition to explosive, tephra-producing eruptions as the edifice builds and water shallows (Jones 1970, Pedersen and Grosse 2014). However, observations in Iceland (Pollock et al. 2014) and in Canada (Edwards et al. 2009) show multiple distinct pillow units separated by deposits of fragmental volcanic material, suggesting a more complicated series of eruptive events and a need for a revised general model of glaciovolcanic, pillow-dominated eruptions. Significant questions also remain regarding the dynamics of magma distribution in the construction of a pillow-dominated glaciovolcanic ridge (tindar). Dikes and lava tubes play important roles in controlling the distribution of lava at mid-ocean ridge pillow edifices (Soule et al. 2007); at Undirhlíðar, a quarry on the Reykjanes Peninsula in southwestern Iceland exposing a cross-section of a tindar,

dikes have been shown to feed pillow units, and irregularly shaped intrusions (massive columnar jointed basalts, MCJBs) may be related to a shallow magmatic plumbing system (Pollock et al. 2014).

While conducting fieldwork along the top of Undirhlíðar tindar in southwestern Iceland we identified pillow-like outcrops of basalt with radial and columnar jointing, concentric bands of vesicles and (where present) glassy rims; however, these outcrops were up to several times larger in cross-sectional dimensions than regular pillows and occurred in high relief from the surrounding pillow units. Although not previously identified at Undirhlíðar, comparable features have been called "megapillows" in Hawaii (Bear and Cas 2007), Tasmania (Goto and McPhie 2004), New Zealand (Bartrum 1930, Walker 1992), Japan (Yamagishi 1991), and British Columbia (Hungerford et al. 2014). These geologists hypothesize that megapillows represent conduits by which lava is fed from the volcanic vent to the advancing pillow front. This raises the question of whether such features are truly mega*pillows* – by definition extrusive and subaqueous – or if they represent intrusive feeder tubes or post-eruption intrusions. Here we report petrographic and geochemical descriptions of nine megapillow outcrops from Undirhlíðar and investigate their role in shallow magmatic plumbing by examining spatial and compositional relationships among megapillows and lava units of the ridge.

Geologic setting

The Reykjanes Peninsula in southwest Iceland connects the Western Volcanic Zone to the slow-spreading Reykjanes Ridge (Fig. 1A). This active, subaerially exposed portion of the mid-ocean ridge system is broken into en echelon NE–SW-trending volcanic segments (from west to east (Fig. 1A) Reykjanes, Krisuvik, Brennisteinsfjöll and Hengil; Jakobsson et al. 1978, Saemundsson 1980). Pleistocene volcanism focused primarily in the present-day volcanic systems produced NE-trending glaciovolcanic ridges reaching elevations of 300–400 m above sea level (Saemundsson et al. 2010; Schopka et al. 2006) that, today, protrude through post-glacial lava fields (Fig. 1). Undirhlíðar and Vatnnskarð quarries are located at the northern extension of the Sveifluhals ridge, which is part of the Krisuvik fissure system (Fig. 1B). Regional mapping has assigned most of the volcanic ridge to the Weichselian (118–10 kyr; Saemundsson et al. 2010), and the northernmost end to the Early Weichselian (118–80 kyr; Lambeck et al. 2006).

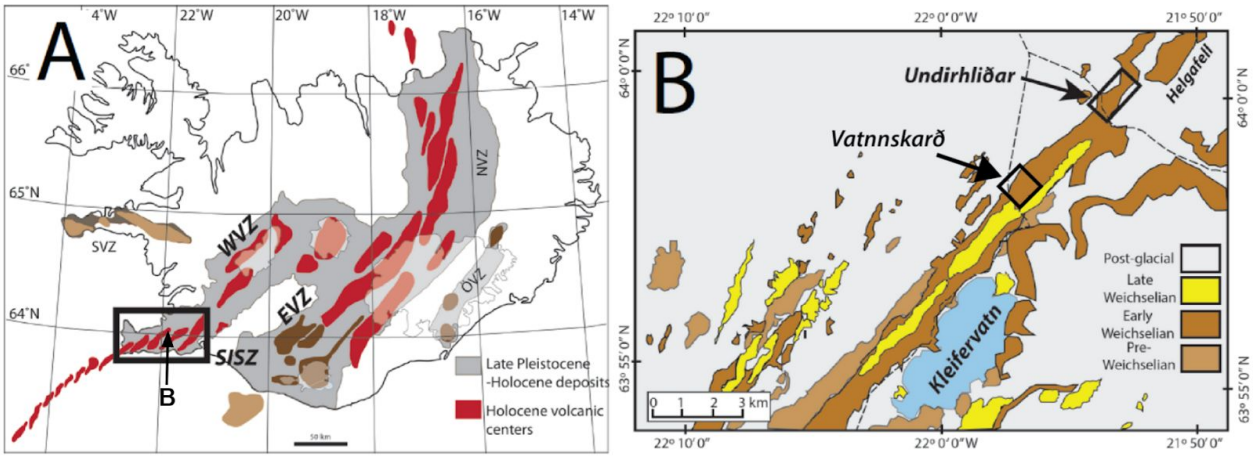

Figure 1 (*above*). **A:** Active volcanic centers in Iceland after Edwards et al. (2012). Box shows Reykjanes Peninsula broken into en echelon NE-SW trending volcanic segments. **B:** At the northeast end of the Krisuvik fissure system on a NE-SW trending glaciovolcanic ridge, boxes highlight locations of Undirhlíðar and Vatnnskarð quarries. Dashed lines indicate roads; area of study lies along the ridge between the two quarries. From Pollock et al. (2014) after Saemundsson et al. (2010).

Site description

On the Reykjanes Peninsula (Fig. 1), quarries ~3 km apart at Undirhlíðar and Vatnsskarð expose cross-sections of a glaciovolcanic tindar, a volcanic ridge formed by fissure eruptions under ice. Pollock et al. (2014) interpret the lithostratigraphic, mineralogical and geochemical variations exposed in the walls of Undirhlíðar quarry and present a model for the formation of the volcanic ridge. They describe Undirhlíðar ridge as a ~150 m thick sequence of interstratified pillow lavas, tuff-breccias and tuffs, and identify eight distinct lithostratigraphic units of coherent and volcaniclastic lithofacies with varying concentrations of plagioclase-olivine-clinopyroxene: four tholeiitic basalt pillow lava units representing four discrete eruptions of low effusion rates, two tuff-breccia fragmental units from two distinct volcaniclastic events, and many larger, massive intrusive bodies of tholeiitic basalt surrounded by tuff lenses. From these observations, Pollock et al. (2014) propose a four-phase model for the formation of Undirhlíðar (Fig. 2); (1) a series of effusive pillow eruptions under relatively thick ice, (2) intrusions through the edifice feeding new effusive fronts and building the ridge, (3) explosive eruption of new magma as water shallows, and (4) a final effusive phase.

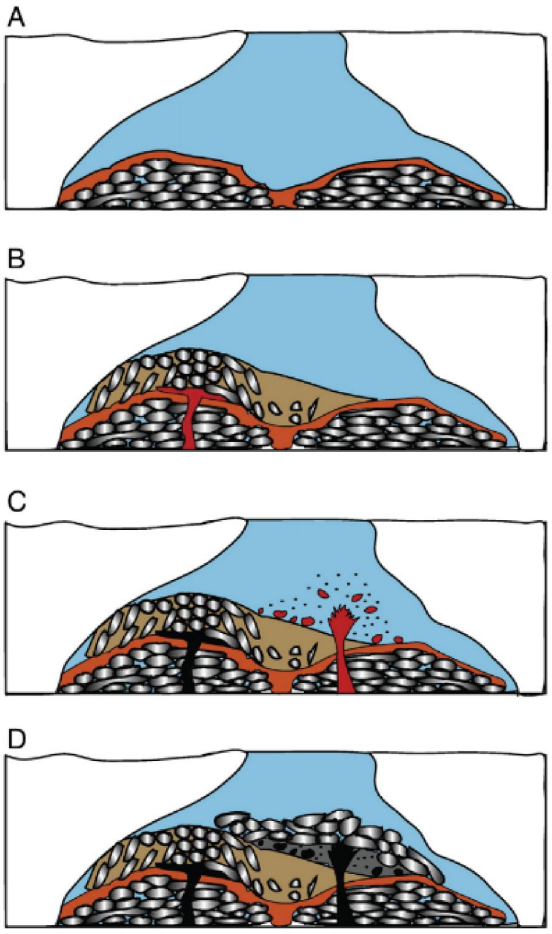

Figure 2. Model for the formation of Undirhlíðar, from Pollock et al. (2014), with glacier (white), sub-glacial lake (blue), pillow lava (gray), pillow breccia (tan), and dikes (magma in red, lava in black).

The research presented here focuses on the previously unstudied ~3 km of the ridge between the two quarries, along the top of which several megapillows are exposed (Fig. 3).

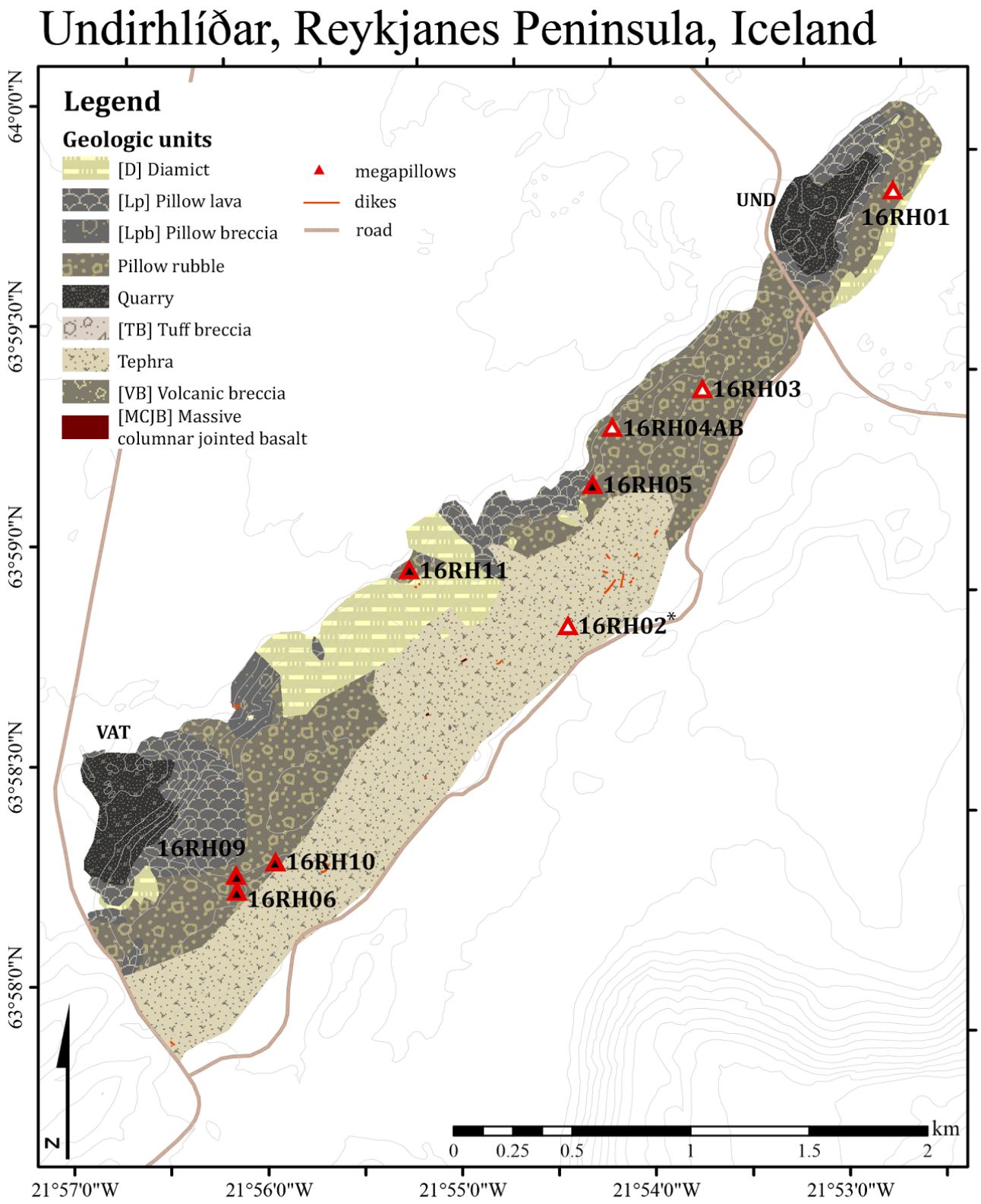

Figure 3. Geologic map of Undirhlíðar showing quarries (UND and VAT), lithologic units, megapillow locations and topography. Megapillows are labeled white for Group 1, black for Group 2 (see Petrography). 16RH02* is unlike other outcrops - see Discussion. 16RH06 also indicates the locations of samples 16RH07 and 16RH08, from the same outcrop.

METHODS

A geologic map of the exposed lithofacies comprising ~3 km of the ridge was constructed using data collected with Trimble Juno handheld GPS units and compiled in ArcGIS (ESRI) with sample locations, topographic contours and nearby roads, shown in the ISN 1993 Lambert Conic Conformal projection. Field work was concentrated along the top of the ridge and outcrops were sampled mostly from 160-225 m above sea level, although sample 16RH11 was taken from an outcrop in a gully on the northwest slope at 115 m a.s.l. Cross-sectional dimensions of selected megapillow outcrops were estimated from field photos in ImageJ.

Fourteen thin sections were created out of twelve rock samples from nine outcrops, representing the crystalline interior of each megapillow as well as features (when present) such as the glassy pillow edge, vesicle bands and regions of alteration. Thin sections were analyzed using standard polarizing light microscopy on a Leica DM750P microscope and photographed on a Leica ICC50 HD camera. Selected samples were also imaged with back-scattered electrons (BSE) analyzed using energy dispersive X-ray spectrometry (EDS) under a TESCAN Vega3 scanning electron microscope with an Oxford X-Max^{N} 80 detector.

For this paper twelve whole-rock geochemical analyses of megapillow samples were acquired. Powders were prepared from the fresh crystalline interiors of megapillows and crushed in alumina ceramic grinding containers. Loss on ignition (LOI) was determined by heating the samples at 950 °C for 1h following the methods of Boyd and Mertzman (1987). Fused glass beads and pressed pellets were prepared and major and minor elements were measured at The College of Wooster by X-ray fluorescence (XRF) spectrometry, all following the methods of Pollock et al. (2014). Low-abundance trace elements were measured by inductively coupled plasma mass spectroscopy (ICP-MS; VG PlasmaQuad 3) at Washington State University. Geochemical analyses of pillow unit, dike, and MCJB samples and MCJB thin sections acquired by Pollock et al. (2014) were used for comparison with new data.

RESULTS

Outcrop descriptions and mapping

Megapillows occur among pillow lava units along the entire length of the field site (Fig. 3). Megapillows vary in size and shape, and are identifiable by their distinctive radial and columnar jointing, concentric bands of vesicles and frequent glassy rims. They consistently occur in relief from surrounding units of basalt breccia below, which is often glassy and resembles pillow rubble (Fig. 4). This is least apparent in outcrop 16RH02, the second outcrop we identified, which is buried in tephra. Megapillows contain visible plagioclase and some olivine and clinopyroxene phenocrysts. Some are very massive and irregular (ex. 16RH04, 16RH11) while others are neatly exposed as round cross-sections of tube-shaped megapillows.

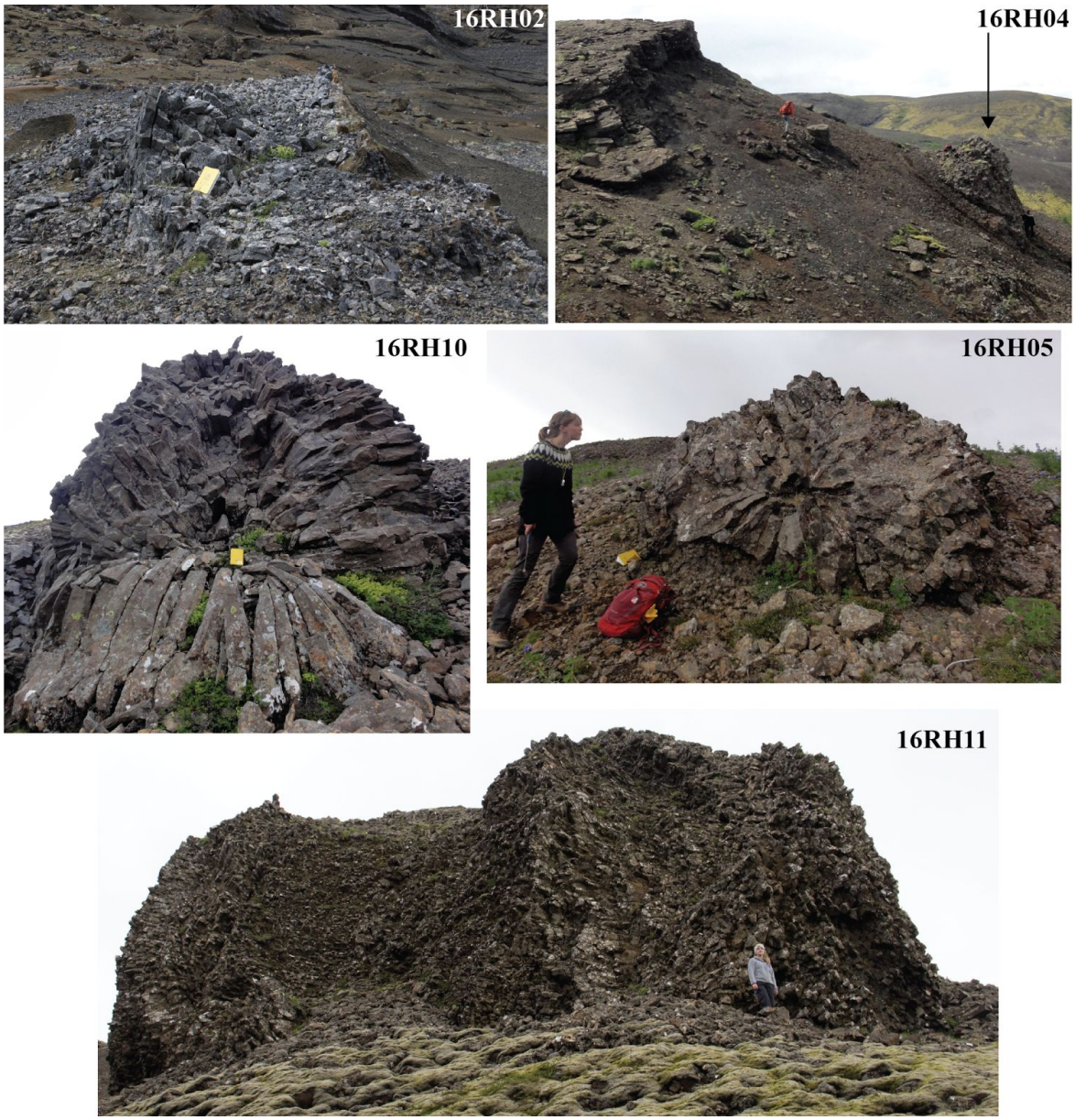

Figure 4. Field photos of some outcrops sampled: 16RH02, 16RH04, 16RH05, 16RH10 and 16RH11. Field notebooks and people for scale; see Figure 3 for outcrop locations. Note radial jointing, irregularity of shape and size, relative enormity, and situation on ridge slope among units of pillow rubble.

Megapillows at Undirhlíðar appeared self-evident due to their high relief and coherence in otherwise unconsolidated pillow rubble, and are quantitatively distinguishable from regular pillows by their size (Fig. 5): Walker's (1992) morphometric study of pillow-size spectrum among pillow lavas measured cross-sections of individual basalt pillows and found dimensions generally less than a meter; however these megapillows are up to several meters in cross-sectional diameter. While pillow lavas in the quarry average cross-sectional horizontal/vertical dimensions of 0.5/0.2 m, these outcrops roughly average 5.3/3.4 m. Those outcrops that fall within the range of regular pillow dimensions occurred fully intact in units of pillow rubble, and showed cross-sectional dimensions well above those of the average pillow.

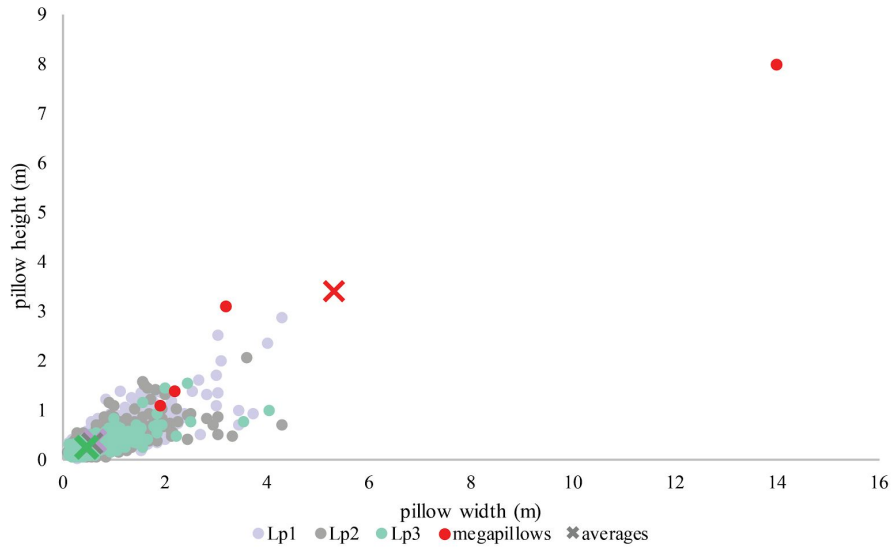

Figure 5. Measured (dots) and average (X) horizontal/vertical dimensions of selected megapillows (red) and pillow lava units of Undirhlíðar: Lp1 (light purple), Lp2 (gray), Lp3 (turquoise). Regular pillows average 0.5/0.2 m (H/V).

Petrography

All the samples analyzed in thin section are vesicular plagioclase-phyric olivine basalts with plagioclase-rich groundmass that fall into two broad groups: **(1)** porphyritic with mostly plagioclase laths, some (<10%) augite and rare (<2%) olivine phenocrysts in a microcrystalline matrix and **(2)** coarser-grained porphyritic with large (up to ~1 mm) plagioclase laths and more (~10-20%) augite and olivine phenocrysts, frequently displaying a subophitic texture (Fig. 6). Among the phenocrysts in both groups were "crystal clots", spherulitic glomerocrysts of plagioclase laths with olivine or augite at the center. Samples in both groups contain up to 5% round opaque oxides. The first group is found mostly towards the northeast end of the ridge, and the second group to the southwest (Fig. 1).

(1) The samples of the first group, 16RH01, 16RH02A/B, 16RH03, and 16RH04A/B, show a bimodal crystal size distribution of up to 15% phenocrysts of ~0.5+ mm, mainly plagioclase or augite and rarely olivine, in a devitrifying microcrystalline plagioclase and augite matrix. Some plagioclase show visible zoning in cross-polarized light. Vesicles are mostly ~0.5-2.0 mm in diameter and make up ~15-30% of the samples. Some of the samples in this group (16RH02A, 16RH04A) contain chrome spinel inclusions.

(2) The second group, containing samples 16RH05, 16RH06, 16RH07, 16RH08A/B, 16RH09, 16RH10 and 16RH11, is coarser-grained and highly crystalline with very little glass. These samples are dominated both in phenocrysts and groundmass by plagioclase laths which show both spherulitic and trachytic textures. Olivine and augite phenocrysts are euhedral, up to ~0.5 mm in diameter and contain opaque oxides and parts of other crystals.

Figure 6. (*Below*) Thin section photos in plane-polarized (left) and cross-polarized (right) light of samples 16RH02A and 16RH04B from petrographic group **(1)** and 16RH05 and 16RH07 from group **(2)**. Note relative grain size and crystal textures of groundmass and phenocrysts, including glomerocrysts, plagioclase laths, phenocryst zoning and devitrification.

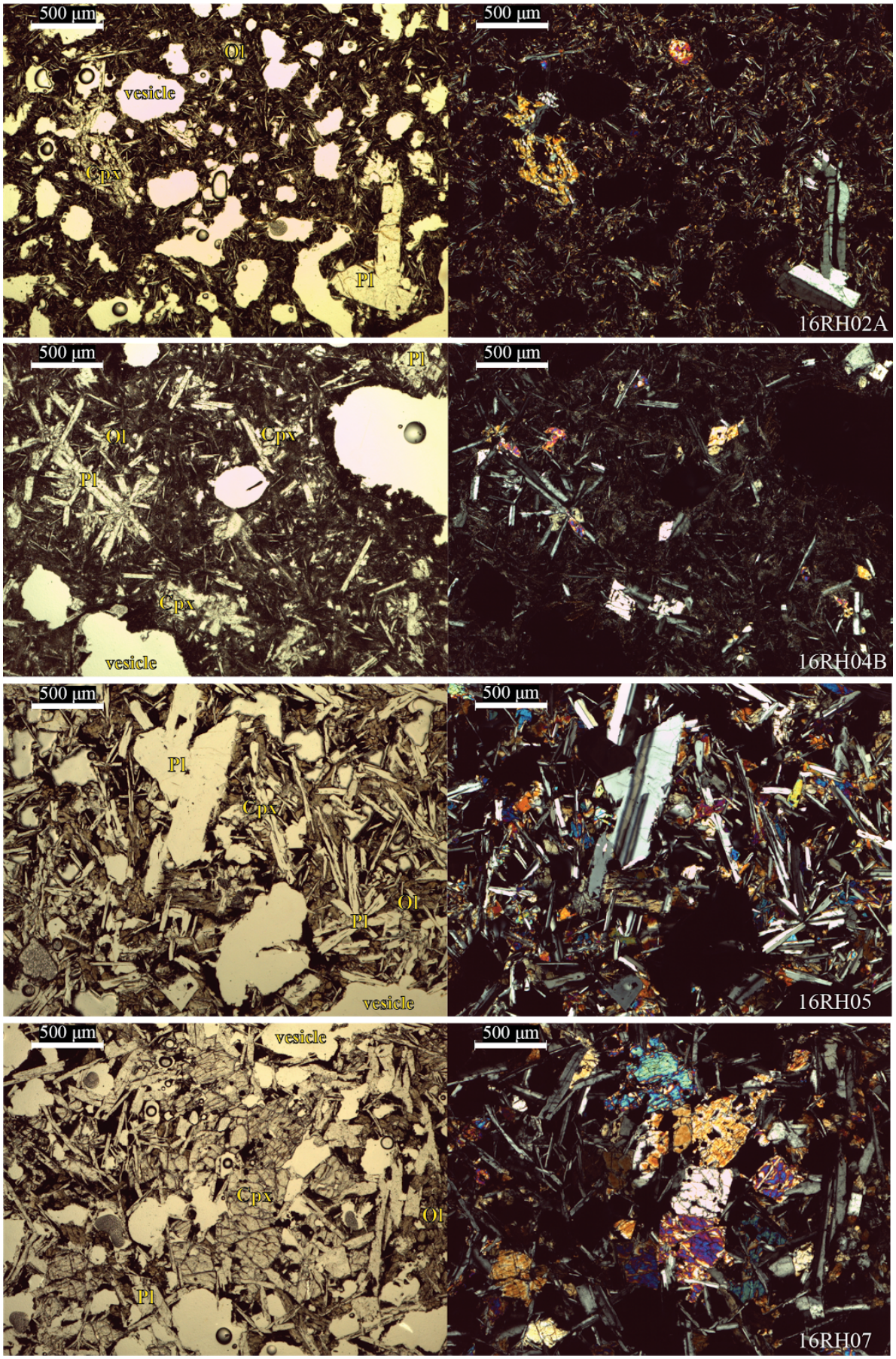
500 µm
Ol
vesicle
Cpx
Pl
16RH02A
500 µm
Pl
Ol
Cpx
Pl
Cpx
vesicle
16RH04B
500 µm
Pl
Cpx
Ol
Pl
vesicle
16RH05
500 µm
vesicle
Cpx
Ol
Pl
16RH07
500 µm

Geochemistry

Sample:	16RH01	16RH02	16RH03	16RH04A	16RH04B	16RH05	16RH06	16RH07	16RH08	16RH09	16RH10	16RH11
SiO2	**48.04**	**49.01**	**47.59**	**47.80**	**47.72**	**48.46**	**48.13**	**48.16**	**48.10**	**48.09**	**48.04**	**49.24**
TiO2	**1.57**	**1.85**	**1.58**	**1.75**	**1.72**	**1.67**	**1.65**	**1.74**	**1.63**	**1.74**	**1.56**	**1.80**
Al2O3	**16.22**	**15.10**	**16.95**	**16.18**	**16.06**	**16.44**	**17.21**	**17.14**	**17.05**	**16.92**	**17.42**	**16.10**
FeO*	**11.60**	**12.71**	**11.10**	**11.64**	**11.67**	**11.44**	**10.89**	**11.14**	**10.94**	**11.23**	**10.78**	**11.49**
MnO	**0.19**	**0.21**	**0.18**	**0.19**	**0.19**	**0.19**	**0.18**	**0.18**	**0.18**	**0.18**	**0.18**	**0.19**
MgO	**8.26**	**7.16**	**8.32**	**8.05**	**8.37**	**7.48**	**7.41**	**7.08**	**7.62**	**7.16**	**7.60**	**6.44**
CaO	**11.61**	**11.12**	**11.80**	**11.89**	**11.81**	**11.67**	**11.85**	**11.81**	**11.85**	**12.04**	**11.80**	**11.82**
Na2O	**2.23**	**2.38**	**2.20**	**2.19**	**2.17**	**2.35**	**2.39**	**2.44**	**2.35**	**2.33**	**2.35**	**2.49**
K2O	**0.14**	**0.26**	**0.13**	**0.14**	**0.14**	**0.16**	**0.14**	**0.15**	**0.14**	**0.15**	**0.14**	**0.25**
P2O5	**0.14**	**0.19**	**0.14**	**0.16**	**0.16**	**0.14**	**0.15**	**0.16**	**0.15**	**0.15**	**0.14**	**0.19**
Sum	**100.00**	**100.00**	**100.00**	**100.00**	**100.00**	**100.00**	**100.00**	**100.00**	**100.00**	**100.00**	**100.00**	**100.00**
LOI	0.00	0.00	0.00	0.00	0.00	0.00	0.00	0.00	0.00	0.00	0.00	0.00
Trace Elements (ppm)												
Sc	37.1	40.8	35.4		38.3	37.2	34.1			37.4	34.0	37.8
V	**321**	**373**	**302**	**344**	**334**	**328**	**305**	**310**	**303**	**324**	**290**	**343**
Cr	**291**	**251**	**298**	**301**	**288**	**258**	**307**	**282**	**287**	**286**	**279**	**112**
Ni	**125**	**94**	**140**	**137**	**131**	**111**	**122**	**112**	**123**	**103**	**116**	**67**
Cu	**125**	**142**	**132**	**101**	**115**	**113**	**134**	**157**	**130**	**141**	**122**	**158**
Zn	**92**	**104**	**90**	**93**	**94**	**90**	**87**	**90**	**88**	**90**	**86**	**94**
Rb	2.0	4.7	1.6	**4.0**	1.6	2.4	1.8	**4.0**	**4.0**	1.9	1.8	4.3
Sr	212	175	226	**220**	222	219	240	**252**	**243**	233	232	224
Y	22.00	28.58	21.24	**24.00**	23.05	22.92	21.68	**23.33**	**21.67**	23.12	20.87	25.81
Zr	70	99	72	**81**	78	75	74	**80**	**76**	77	71	97
Nb	8.16	12.56	8.94	**12**	9.8	9.0	9.2	**12**	**11**	9.60	8.81	13.52
Cs	0.02	0.05	0.02		0.02	0.03	0.02			0.02	0.01	0.06
Ba	43	71	43	**42**	44	49	46	**51**	**45**	44	44	77
La	6.25	9.38	6.38		6.81	6.69	6.74			7.17	6.59	10.24
Ce	15.02	22.22	15.89		17.02	16.24	16.31			17.28	15.73	23.42
Pr	2.24	3.21	2.33		2.48	2.42	2.42			2.55	2.34	3.28
Nd	10.78	14.54	11.18		11.99	11.40	11.61			12.04	11.22	15.17
Sm	3.13	4.18	3.23		3.61	3.32	3.28			3.51	3.15	4.05
Eu	1.27	1.55	1.28		1.34	1.33	1.30			1.36	1.27	1.51
Tb	0.68	0.88	0.68		0.74	0.70	0.68			0.73	0.66	0.80
Gd	3.92	4.92	3.87		4.09	4.14	3.95			4.17	3.76	4.63
Dy	4.27	5.53	4.28		4.50	4.58	4.27			4.47	4.12	4.99
Ho	0.89	1.16	0.87		0.92	0.94	0.88			0.93	0.85	1.04
Er	2.37	3.15	2.30		2.51	2.50	2.33			2.47	2.27	2.75
Tm	0.33	0.45	0.32		0.36	0.36	0.33			0.35	0.32	0.40
Yb	2.09	2.83	1.99		2.16	2.20	2.03			2.13	1.97	2.42
Lu	0.32	0.44	0.31		0.34	0.34	0.31			0.32	0.31	0.38
Hf	1.94	2.69	1.96		2.16	2.06	2.00			2.11	1.94	2.60
Ta	0.52	0.80	0.56		0.60	0.58	0.58			0.61	0.55	0.86
Pb	0.48	0.76	0.47		0.47	0.52	0.45			0.43	0.43	0.73
Th	0.34	0.66	0.30		0.33	0.37	0.31			0.31	0.30	0.70
U	0.10	0.20	0.10		0.10	0.12	0.10			0.10	0.10	0.22
Calculated values												
La_N/Sm_N	2.00	2.24	1.98		1.89	2.01	2.06			2.04	2.09	2.53
Eu/Eu*	1.11	1.05	1.10		1.06	1.09	1.10			1.08	1.12	1.06

Table 1. Major oxide (wt.%) and trace element (ppm) abundances for megapillow samples measured by XRF (bold) and ICP-MS (regular font). La_N/Sm_N and Eu/Eu* were calculated using abundances normalized to chondrite values in Sun and McDonough (1989).

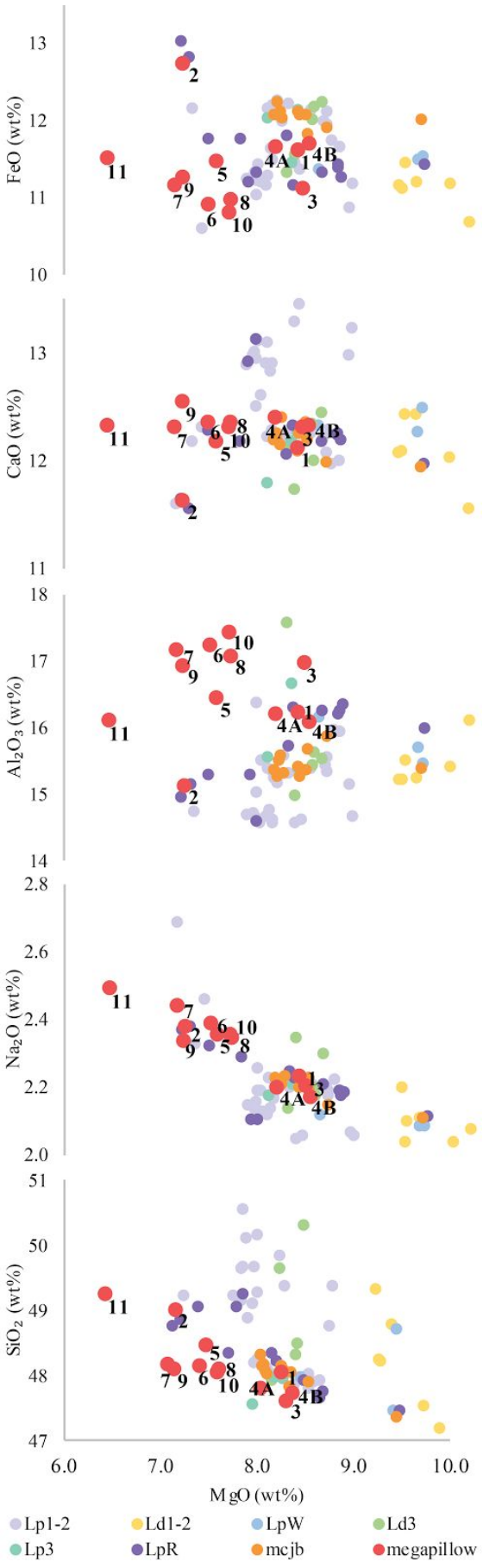

Twelve whole-rock geochemical analyses of megapillow samples were acquired (Table 1) and compared with analyses of pillow lava units on the ridge, those of the pillow units and dikes of Undirhlíðar reported by Pollock et al. (2014), and of MCJBs from Vatnsskarð (Fig. 7).

Megapillows are generally lower in MgO (6.4-8.4 wt.%) and higher in Al_2O_3 (7.2-17.4 wt.%) and Na_2O (2.2-6.4 wt.%) than the other lava units of the ridge and quarries.

The two petrographic groups are also geochemically distinct. Group **(1)** samples 1, 3, 4A and 4B are geochemically very pillow-like; these samples are higher in MgO, representing a more primitive magma composition. Group **(1)** is also similar to the MCJBs of Vatnsskarð, but MCJBs show higher FeO and lower Al_2O_3 than megapillows. Sample 16RH02 is geochemically dissimilar to its petrographic group: it is lower than the other group **(1)** samples in MgO and very high in FeO. The more crystalline group **(2)** samples are lower in MgO and higher in Al_2O_3 (i.e. 16RH10), indicating a more evolved magma. Sample 16RH11 does not show the elevated Al_2O_3 of the rest of its group and is especially low in MgO.

Figure 7. (*Left*) Major element plots of wt.% MgO (*x*) vs. wt.% major oxides FeO, CaO, Al_2O_3, Na_2O, SiO_2 (*y*) for megapillows (red, sample numbers to lower right), MCJBs (orange), Undirhlíðar pillow units Lp1-2 (light purple), Lp3 (turquoise), LpW (light blue), dikes Ld1-2 (yellow), Ld3 (light green), and ridge pillow units, LpR (purple).

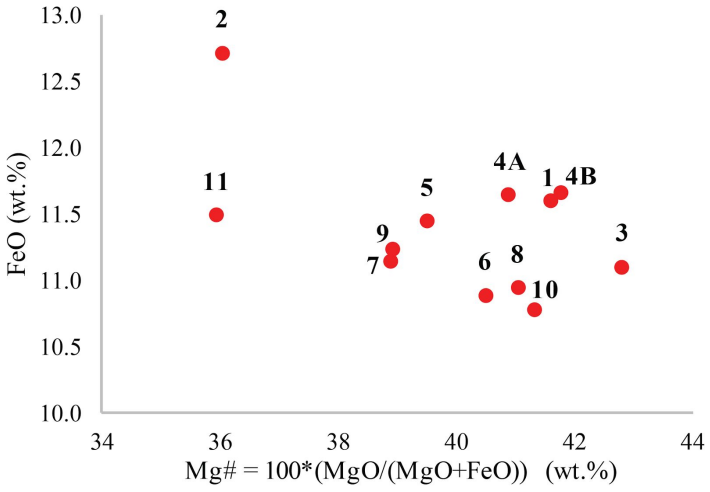

Figure 8. (*Above)* Wt.% FeO* vs. Mg# for megapillows.

Megapillows range in Mg# from 38.8-42.8 (Fig. 8), except for samples 16RH02 and 16RH11 (Mg# ~36).

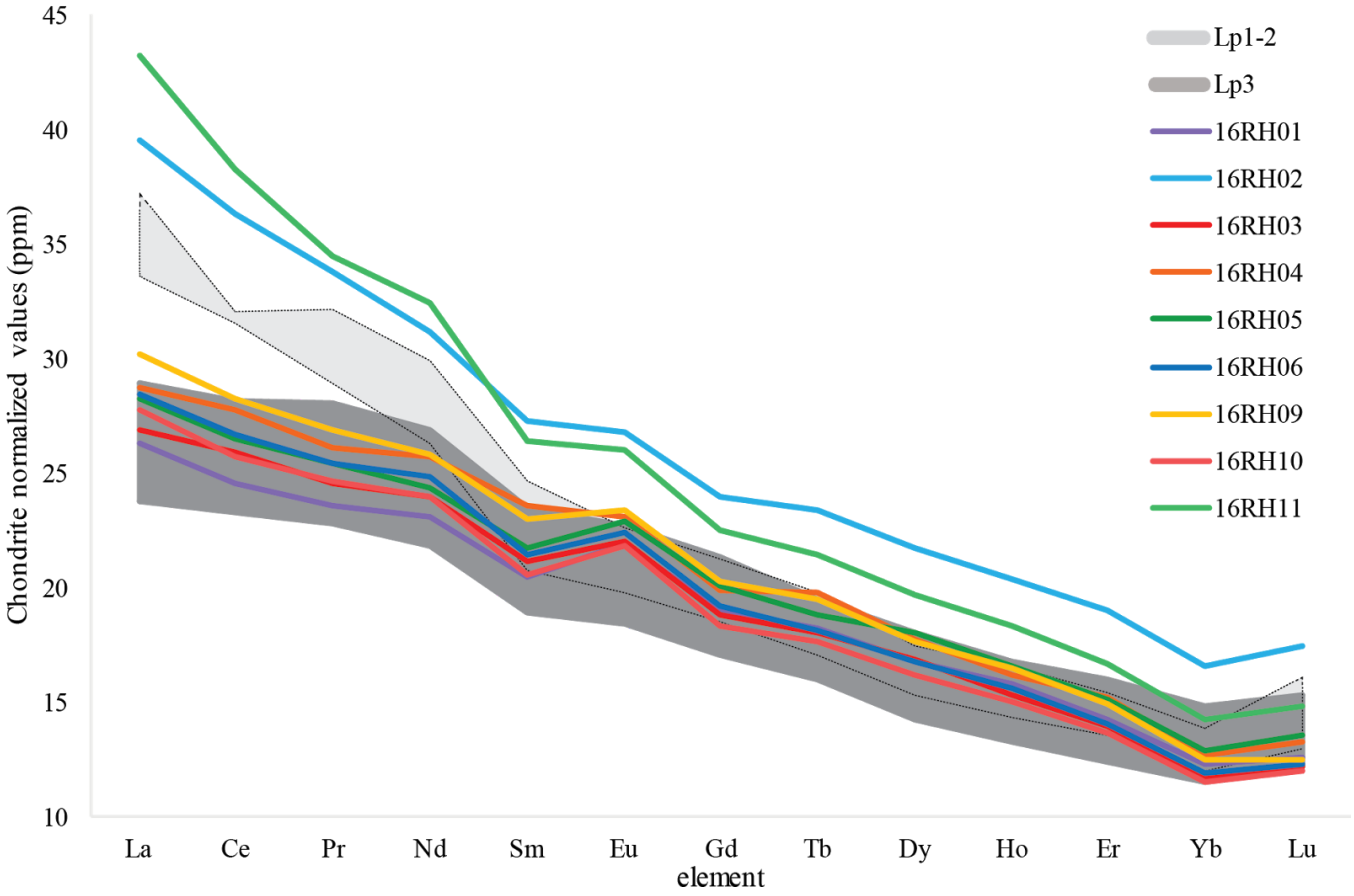

Figure 9. Chondrite-normalized (chondrite values from Sun & McDonough 1989) rare earth element diagrams showing elemental abundances (ppm) in megapillows and ranges of pillow lava units from two distinct magma batches, Lp1-2 (light gray/dashed border) and Lp3 (dark gray), in Undirhlíðar (Pollock et al. 2014).

Rare earth element abundance patterns for most megapillows (Fig. 9) are very similar to one another and to the upper pillow unit (Lp3) identified by Pollock et al. (2014) in Undirhlíðar quarry. Unlike pillow units, megapillows show strong positive Eu anomalies (average Eu/Eu* = 1.1) (Table 1).

16RH02 and 16RH11 are significantly enriched as compared to other megapillows and to the units at Undirhlíðar, 16RH11 even more so in the lighter rare earth elements. Of nine megapillow samples for which La_N/Sm_N was calculated, seven fall within the range of La_N/Sm_N = 1.22-1.35 (Table 1). Samples 16RH02 and 16RH11 show elevated La_N/Sm_N ratios of 1.45 and 1.63, respectively. Pollock et al. (2014) identified two trace element populations; those of incompatible element-depleted Lp1-2 (La_N/Sm_N = ~1.3) and enriched Lp3 (La_N/Sm_N = ~1.6). 16RH11 falls within the range of Lp1-2 La_N/Sm_N values; 16RH02 is between the two ranges; all other megapillows are within the trace element range of Lp3.

Mineral compositions

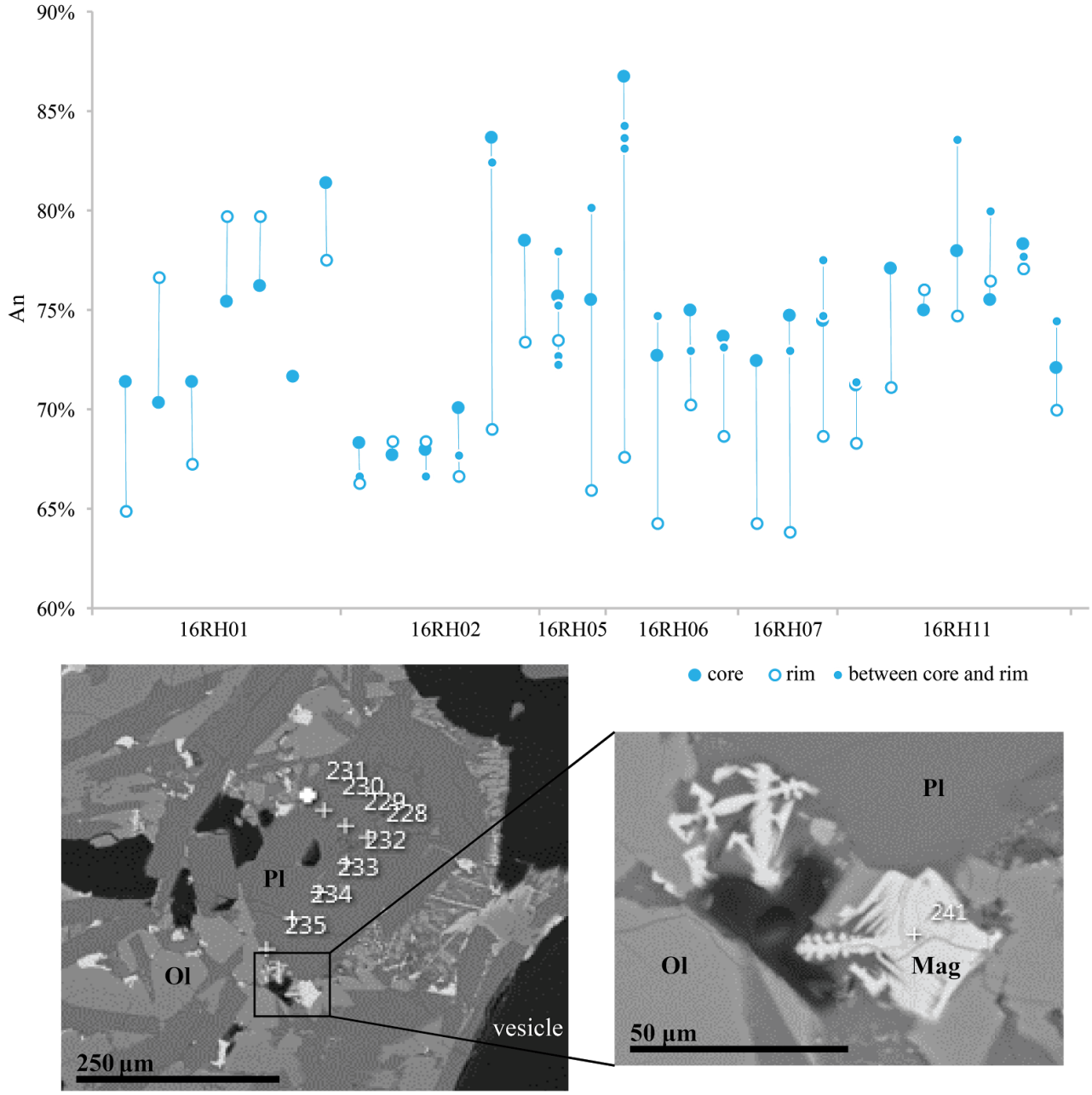

Figure 10. Plagioclase phenocryst compositions and thin section electron images. *Above*: Plot of measured An values from core to rim of 29 plagioclase phenocrysts from six samples. Filled circle indicates a point located at the core, open circle at the rim, smaller filled dot between the core and rim. *Below*: Electron images of sample 16RH05 show locations of acquired spectra, bright Fe-rich edges of zoned olivine phenocrysts, and dendritic interstitial Fe-Ti oxide texture.

Elemental compositions of selected phenocrysts and oxides in thin sections of samples from both petrographic groups, 16RH01 & 16RH02 **(1)** and 16RH05, 16RH06, 16RH07 and 16RH11 **(2)**, were used to estimate major cations, determine An/Ab for plagioclase and Fo/Fa for olivine phenocrysts and examine zoning within crystals. Plagioclase compositions among the selected samples range from An64 to An87 with an average of An73; this is consistent with the phenocryst compositions measured by Pollock et al. (2014) in Undirhlíðar

pillow units. Core and rim analyses of individual crystals showed varied zoning patterns (Fig. 10); small shifts in measured composition may be due to analytical error but most phenocrysts showed definitive zoning with a >10% change in composition. Phenocrysts in samples 16RH06 and 16RH07 were normally zoned, with higher-An cores, while other samples show reverse (ex. 16RH01, 16RH02) or oscillatory (ex. 16RH05, 16RH11) zoning.

Olivine phenocrysts showed visibly bright, Fe-rich rims in electron images (Fig. 10). Calculated Fo values averaged Fo54 at the rims of olivine phenocrysts, compared to Fo80 for cores. Interstitial dendritic oxides of ~50-100 μm across are shown by composition to be Ti-rich magnetites.

DISCUSSION

The most conspicuous characteristic of megapillows is their size. Pillow dimensions are primarily controlled by magma composition, effective viscosity and supply rate (Walker 1992; Bear and Cas 2007). Megapillows, like other Undirhlíðar lavas are tholeiitic basalts (Pollock et al. 2014), but their effective viscosity relative to pillows of similar composition can be affected by crystallinity (Walker 1992); based on the Einstein-Roscoe equation, the relative viscosities of phenocryst-bearing magmas with 30 vol.% and 50 vol.% phenocrysts are $10^{0.8}$ and $10^{2.0}$, respectively (Takeguchi 2011). Elevated wt% Al_2O_3 and a strong Eu anomaly in whole-rock analyses sets megapillows apart from other lavas of the ridge and suggests significant plagioclase phenocryst accumulation (Crawford et al. 1987). Within megapillows, the highly crystalline samples of petrographic group **(2)** show higher wt% Al_2O_3 (with the exception of 16RH11) than group **(1)**; the outcrops of group **(2)** are also much larger than group **(1)** with the exception of 16RH04, The presence of a large volume of plagioclase crystal cargo, buoyant under pressure in dense magma, would increase the effective viscosity of that magma body, enabling formation of larger pillows. However, Gregg and Smith (2003) argue that it often requires order of magnitude changes in viscosity to change lava morphology, and that viscosity alone cannot dictate morphology; investigation of effusion rates of megapillow eruption is needed to address the question of their size.

By definition, a mega*pillow* represents the product of extrusive, subaqueous eruption, rather than an intrusive conduit (such as a lava tube) or a post-eruption intrusion. The Undirhlíðar megapillows' glassy margins, vesicle bands and radial and columnar jointing are features consistent with true pillows; however, this does not preclude their role in magmatic distribution. In Tasmania, pillows are shown radially propagating from the basal margins of a fully exposed marine megapillow at Plum Pudding Rock (Goto and McPhie 2004). In British Columbia a large glaciovolcanic pillow is observed with smaller pillows propagating from its base (Edwards et al. 2009, Fig. 4). Goto and McPhie (2004) note theirs is the only known three-dimensional exposure of a megapillow; it likely remains the most pristine example. They argue for a style of subaqueous pillow propagation in which pillows emerge and are fed from the base of megapillows (and/or sheet flows) which then override them, creating an upward gradation from pillow into massive lavas. The megapillows at Undirhlíðar, while exposed in three dimensions, are eroded and lie within a complex stratigraphic sequence of glaciovolcanic and later glacial material. They occur in contact with pillow rubble at their base, and although intact pillows are not apparent, they

are geochemically and genetically related to the pillow units in which they are found; this is consistent with Goto and McPhie's (2004) model. The accumulation of plagioclase in megapillows may therefore be the result of dense, liquid magma filtering down out of the buoyant plagioclase phenocryst-rich interior of the megapillow and preferentially flowing into the pillows developing from its base. This hypothesis can be further tested by modeling the addition of measured plagioclase phenocryst compositions to regular pillow compositions.

Irregular zoning of plagioclase phenocrysts in 16RH01, 16RH02 and 16RH11 suggests they developed in an environment that was saturated by multiple, diverse pulses of magma. Megapillows' high volume-to-cooling-surface ratio induces a slower rate of magma cooling and crystallization, which could allow megapillows to serve for some time as sustained liquid conduits; the movement of pulses of magma throughout such a crystal-rich conduit would lead to irregular phenocryst zoning. The megapillow near Vatnsskarð represented by samples 16RH06 (margin) and 16RH07 (interior) shows normal plagioclase zoning, suggesting phenocryst growth during crystallization of a magma body cooling in place undisturbed. Fe-rich olivine rims and interstitial dendritic Fe-Ti oxides appear to have developed later from the last Fe-rich drops of a mostly frozen magma.

Megapillows appear petrographically consistent with the pillow units of Undirhlíðar described by Pollock et al. (2014). Of the two petrographic groups, group **(2)** is distinguishable from regular pillow units by visibly higher crystallinity; group **(1)** is similar to regular pillows. These groups are also geographically and geochemically distinct: group **(1)** occurs at the northeastern end of the ridge, close to Undirhlíðar quarry, and with the exception of 16RH02, these outcrops are more primitive than group **(2)**, which occurs to the southwest near Vatnsskarð with a more evolved composition and generally higher wt% Al_2O_3.

Sample 16RH11 stands out as magnesium-poor, incompatible element-enriched, weak in Eu anomaly, and an exception within its petrographic group in major element composition. It's the lowest-elevation megapillow sampled, exposed in a gully ~100 m below the other megapillows. Its La_N/Sm_N ratio of 1.63 lies at the upper end of a range previously only measured in the basal pillow units (Lp1-2) of Undirhlíðar (Pollock et al. 2014); this suggests it formed with those units during an earlier phase of eruption. The rest of the megapillows fall near or within the less-enriched range of upper Undirhlíðar and Vatnsskarð pillow units (Lp3, $La_N/Sm_N = 1.28\pm0.4$) that Pollock et al. (2014) interpret to represent a later magma batch distinct from the first, and likely formed from this magma. The difference between the two groups' textures and geochemistry is thus a result of differentiation of that magma to produce the more primitive group **(1)** and evolved group **(2)**; the spatial distribution of these groups may be related to the extent of the tephra cone, whose northeastern end marks their divide. Megapillows appear compositionally consistent with multiple eruptive events in the construction of the ridge; however an investigation of isotopic data in megapillows is needed to verify the hypothesis of multiple magma sources.

Sample 16RH02 is even more out of place. It was initially identified as a megapillow due to its radial columnar jointing, concentric vesicle bands and glassy margins; however it occurs within a tephra unit, rather than the pillow rubble in which we found every other megapillow. It's possible that a megapillow outcrop could be partially buried by ashfall and protrude through the eroded tephra cone as 16RH02 did, but it's also unlike

megapillows geochemically: it's far higher in Fe than any other outcrop and much lower in Mg than the other samples of its petrographic group. In addition, its La_N/Sm_N ratio of 1.45 is not found anywhere else among megapillows or in the quarry units. This leads me to believe that we misinterpreted the outcrop and it should not be classified as a megapillow, but studied within the context of the tephra cone and an explosive eruptive stage.

Pollock et al. (2014) identify a dike in the wall of Undirhlíðar quarry that cuts through a tuff unit to feed an overlying pillow mound (Pollock et al. 2014 Fig. 3C); this mechanism is represented in their eruptive model by the intrusive magma conduits of Phase 2 (Fig. 2B). Megapillows represent a different, extrusive means of magma transport, and rather than cross-cutting other units, occur within the pillow mounds with which they form. Sample 16RH11's geochemical similarity to units Lp1 and Lp2 (Fig. 9) and the lower elevation of that outcrop suggests it formed during Phase 1 or 2 (Fig. 2A, 2B) of the eruption as part of a pillow mound, some of which may have propagated from its margins. The explosive Phase 3 (Fig. 2C) would not have produced megapillows, but the switch of eruptive style back to effusive in Phase 4 (Fig. 2D) likely generated the megapillow units found along the top of the ridge, which played a role in building units Lp3/LpW through pillow propagation at their bases.

CONCLUSIONS

Glaciovolcanic megapillows occur along the length of Undirhlíðar tindar. They are found in multiple pillow units and are genetically and petrographically related to the pillow lavas in which they are found, although significant plagioclase phenocryst accumulation in megapillows is absent in regular pillows. Megapillows appear to have formed during the multiple effusive stages of ridge-building eruption proposed by Pollock et al. (2014) and may be derived from multiple batches of magma. The megapillows at the top of the ridge fall into two petrographic groups: one near Undirhlíðar quarry with a primitive composition and one near the tephra cone representing a more evolved batch of the same magma. Pillow rubble surrounds the outcrops and plagioclase phenocrysts record changing magmatic conditions; this is consistent with Goto and McPhie's (2004) model for pillow propagation from the base of megapillows, resulting in an upward gradation from pillow to massive (megapillow) facies. Megapillows at Undirhlíðar may serve as sustained magmatic conduits, representing a mechanism for extrusive magmatic distribution in which pillows propagate and are fed from their basal margins and are then overrun by the advancing megapillow at the eruptive front.

ACKNOWLEDGEMENTS

I thank my Keck mentors Meagen Pollock and Ben Edwards for all their guidance throughout this project and Zeb Page and Amanda Schmidt for their advising in research and thesis-writing. Thank you to The College of Wooster Geology Department for use of their geochemistry lab and to Oberlin College Department of Geology for SEM assistance and supporting travel for a wonderful GSA experience. This project was supported by the Keck Geology Consortium, ExxonMobil Corporation, and The National Science Foundation (NSF-REU1358987).

REFERENCES

Barendegt, R.W. and Irving, E., 1998, Changes in the extent of North American ice sheets during the Late Cenozoic: Canadian Journal of Earth Science, vol. 35, p. 504–509.

Bartrum, J.A., 1930, Pillow lavas and columnar fan structures at Muriwai Auckland: Journal of Geology vol. 38, no. 5, p. 447–455.

Batiza, R. and White, J.D., 2000, Submarine lavas and hyaloclastite: Encyclopedia of Volcanoes p. 361-381

Bear, A.N. and Cas, R.A.F., 2007, The complex facies architecture and emplacement sequence of a Miocene submarine mega-pillow lava flow system, Muriwai, North Island, New Zealand: Journal of Volcanology and Geothermal Research, vol. 160, p. 1-22.

Boyd, F.R., and Mertzman, S.A., 1987, Composition and structure of the Kaapvaal Lithosphere, Southern Africa: Special Publications Geochemical Society, vol. 1, p. 13-24.

Crawford, A.J., Falloon, T.J. and Eggins, S., 1987, The origin of island arc high-alumina basalts: Contributions to Mineralogy and Petrology, vol. 97, p. 417-430.

Edwards, B.R., Skilling, I.P., Cameron, B., Haynes, C., Lloyd, A., and Hungerford, J.H.D., 2009, Evolution of an englacial volcanic ridge: Pillow Ridge tindar, Mount Edziza volcanic complex, NCVP, British Columbia, Canada: Journal of Volcanology and Geothermal Research, vol. 185, no. 4, p. 251-275.

Fulton, R.J., 1992, Stratigraphy and paleomagnetism of Brunhes and Matuyama (>790 ka) Quaternary deposits at Merritt, British Columbia: Canadian Journal of Earth Sciences, vol. 29, p. 76–92.

Furnes, H., de Wit, M., Staudigel, H., Rosing, M., and Muehlenbachs, K., 2007, A vestige of Earth's oldest ophiolite: Science, vol. 315, p. 1704-1707, doi: 10.1126/science.1139170.

Goto, Y. and McPhie, J., 2004, Morphology and propagation styles of Micoene submarine basanite lavas at Stanley, northwestern Tasmania, Australia: Journal of Volcanology and Geothermal Research, vol. 130, p. 307-328.

Gregg, T.K.P., Smith, D.K., 2003, Volcanic investigations of the Puna Ridge, Hawaii, relations of lava flow morphologies and underlying slopes: Journal of Volcanology and Geothermal Research, vol. 126, p. 63-77.

Höskuldsson, A., Sparks, R.S.J., and Carroll, M.R., 2006: Constraints on the dynamics of subglacial basalt eruptions from geological and geochemical observations of Kverkfjöll, NE-Iceland: Bull Volcanol, vol. 68, p. 689-701.

Hungerford, J.D.G., Edwards, B.R., Skilling, I.P., and Cameron, B.I., 2014, Evolution of a subglacial basaltic lava flow field: Tennena volcanic center, Mount Edziza volcanic complex, British Columbia, Canada: Journal of Volcanology and Geothermal Research, vol. 272, p. 39-58.

Jackson, L.E., Barendregt, R.W., Baker, J. and Irving, E., 1996, Glacial history of the central Yukon: new evidence from field studies and paleomagnetism: Canadian Journal of Earth Science, vol. 33, p. 904–916.

Jakobsson, S.P., Jónsson, J. and Shido, F., 1978, Petrology of the western Reykjanes Peninsula, Iceland: Journal of Petrology, vol. 19, no. 4, p. 669–705.

Johns, S.M., Helmstaedt, H.H. and Kyser, T.K., 2006, Paleoproterozoic submarine intrabasinal rifting, Baffin Island, Nunavut, Canada: volcanic structure and geochemistry of the Bravo Lake Formation: Canadian Journal of Earth Sciences, vol. 43, no. 5, p. 593–616.

Jones, J.G., 1969, Intraglacial volcanoes of the Laugarvatn Region, Southwest Iceland, I: Journal of the

Geological Society of London, vol. 124, p. 197–211.

Jones, J.G., 1970, Intraglacial volcanoes of the Laugarvatn Region, Southwest Iceland, II: Journal of Geology, vol. 78, p. 127–140.

Lambeck, K., Purcell, A., Funder, S., Kjaer, K.H., Larsen, E., and Moller, P., 2006, Constraints on the Late Saalian to early Middle Weichselian ice sheet of Eurasia from field data and rebound modeling: Boreas vol. 35, p. 539–575.

McClintock, M., White, J.D.L., Houghton, B.F., and Skilling, I.P., 2008, Physical volcanology of a large crater-complex formed during the initial stages of Karoo flood basalt volcanism, Sterkspruit, Eastern Cape, South Africa: Journal of Volcanology and Geothermal Research, vol. 172, no. 1–2, p. 93–111.

Pedersen, G.B.M. and Grosse, P., 2014, Morphometry of subaerial shield volcanoes and glaciovolcanoes from Reykjanes Peninsula, Iceland: Effects of eruption environment: Journal of Volcanology and Geothermal Research, vol. 282, p. 115-133.

Pollock, M., Edwards, B., Hauksdóttir, S., Alcorn, R., and Bowman, L., 2014, Geochemical and lithostratigraphic constraints on the formation of pillow-dominated tindars from Undirhlíðar quarry, Reykjanes Peninsula, southwest Iceland: Lithos, v. 200-201, p. 317-333, doi:10.1016/j.lithos.2014.04.023.

Saemundsson, K., Einarsson, S., 1980, Geological map of Iceland, sheet 3, SW Iceland: Museum of Natural History and the Iceland Geodetic Survey, Reykjavik.

Saemundsson, K., Jóhanneson, H., Hjartarson, Á. and Kristinssson, S.G., 2010, Geological map of southwest Iceland, 1:100,000: Iceland GeoSurvey.

Schopka, H.H., Gudmundsson, M.T., and Tuffen, H., 2006, The formation of Helgafell, southwest Iceland, a monogenetic subglacial hyaloclastite ridge: sedimentology, hydrology and volcano-ice interaction: Journal of Volcanology and Geothermal Research, vol. 152, no. 3-4, p. 359-377.

Soule, S.A., Fornari, D.J., Perfit, M.R., and Rubin, K.H., 2007, New insights into mid-ocean ridge volcanic processes from the 2005–2006 eruption of the East Pacific Rise, 9°46′N–9°56′N: Geology, vol. 35, no. 12, p. 1079–1082.

Sun, S. S., and McDonough, W. S., 1989, Chemical and isotopic systematics of oceanic basalts: implications for mantle composition and processes: Geological Society, London, Special Publications, vol. 42, no. 1, p. 313-345.

Takeuchi, S., 2011, Preeruptive magma viscosity: An important measure of magma eruptibility: J. Geophys. Res., vol. 116, B10201, doi:10.1029/2011JB008243.

Walker, G. P. L., 1992, Morphometric study of pillow-size spectrum among pillow lavas: Bull Volcanol, vol 54, p. 459-474.

Yamagishi, H., 1991, Morphological features of Miocene submarine coherent lavas from the ‘Green Tuff’ basins: examples from basaltic and andesitic rocks from the Shimokita Peninsula, northern Japan: Bull Volcanol, vol. 53, p. 173-181.